Title

Triiodothyronine and dexamethasone alter potassium channel expression and promote electrophysiological maturation of human-induced pluripotent stem cell-derived cardiomyocytes

Authors

Wang, Lili
Wada, Yuko
Ballan, Nimer
et al.

Publication Date

2021-12-01

DOI

10.1016/j.yjmcc.2021.08.005

Peer reviewed

HHS Public Access

Author manuscript

J Mol Cell Cardiol. Author manuscript; available in PMC 2023 January 03.

Published in final edited form as:

J Mol Cell Cardiol. 2021 December ; 161: 130–138. doi:10.1016/j.yjmcc.2021.08.005.

Triiodothyronine and dexamethasone alter potassium channel expression and promote electrophysiological maturation of human-induced pluripotent stem cell-derived cardiomyocytes

Lili Wang[1,*], **Yuko Wada**[1], **Nimer Ballan**[2], **Jeffrey Schmeckpeper**[1], **Jijun Huang**[3], **Christoph Daniel Rau**[3], **Yibin Wang**[3], **Lior Gepstein**[2,4], **Bjorn C. Knollmann**[1,*]

[1]Department of Medicine, Vanderbilt University Medical Center, Nashville, TN, Medical Research Building IV, Rm.1275, 2215B Garland Ave, Nashville, TN 37232, USA

[2]Rappaport Faculty of Medicine, Technion-Israel Institute of Technology, POB 9649, Haifa 3109601, Israel

[3]Department of Anesthesiology, Medicine and Physiology, David Geffen School of Medicine, University of California at Los Angeles, Los Angeles, CA, USA

[4]Cardiology Department, Rambam Health Care Campus, Rappaport Faculty of Medicine, Technion – Israel Institute of Technology, 2 Efron St. POB 9649, Haifa, 3109601, Israel

Abstract

Background—Human-induced pluripotent stem cell-derived cardiomyocytes (hiPSC-CMs) have emerged as a promising tool for disease modeling and drug development. However, hiPSC-CMs remain functionally immature, which hinders their utility as a model of human cardiomyocytes.

Objective—To improve the electrophysiological maturation of hiPSC-CMs.

Methods and Results—On day 16 of cardiac differentiation, hiPSC-CMs were treated with 100 nmol/L triiodothyronine (T3) and 1 μmol/L Dexamethasone (Dex) or vehicle for 14 days. On day 30, vehicle- and T3+Dex-treated hiPSC-CMs were dissociated and replated either as cell sheets or single cells. Optical mapping and patch-clamp technique were used to examine the electrophysiological properties of vehicle- and T3+Dex-treated hiPSC-CMs. Compared to vehicle, T3+Dex-treated hiPSC-CMs had a slower spontaneous beating rate, more hyperpolarized resting membrane potential, faster maximal upstroke velocity, and shorter action potential duration. Changes in spontaneous activity and action potential were mediated by decreased hyperpolarization-activated current (I_f) and increased inward rectifier potassium currents (I_{K1}), sodium currents (I_{Na}), and the rapidly and slowly activating delayed rectifier potassium currents (I_{Kr} and I_{Ks}, respectively). Furthermore, T3+Dex-treated hiPSC-CM cell sheets (hiPSC-CCSs) exhibited a faster conduction velocity and shorter action potential duration than the vehicle. Inhibition of I_{K1} by 100 μM $BaCl_2$ significantly slowed conduction velocity and prolonged

[*]Correspondence to: Lili Wang, Ph.D., Division of Clinical Pharmacology, Vanderbilt University Medical Center, Medical Research Building IV, Rm.1275, 2215B Garland Ave, Nashville, TN 37232-0575 lili.wang@vumc.org Or Bjorn C. Knollmann, MD, Ph.D., Vanderbilt Center for Arrhythmia Research and Therapeutics (VanCART), Vanderbilt, University Medical Center, Medical Research Building IV, Rm. 1265, 2215B Garland Ave, Nashville, TN 37232-0575, bjorn.knollmann@vanderbilt.edu.

action potential duration in T3+Dex-treated hiPSC-CCSs but had no effect in the vehicle group, demonstrating the importance of I_{K1} for conduction velocity and action potential duration.

Conclusion—T3+Dex treatment is an effective approach to rapidly enhance electrophysiological maturation of hiPSC-CMs.

Keywords

HiPSC-CMs; T3+Dex treatment; electrophysiological maturation; potassium currents; action potential; conduction velocity

1. Introduction

The human-induced pluripotent stem cell (hiPSC) technology opens new avenues for human disease modeling and drug screening. HiPSC-derived cardiomyocytes (hiPSC-CMs) can recapitulate the structure and function of adult cardiomyocytes (CMs): (1) express cardiac-specific markers, sarcomere proteins, and calcium handling regulators [1–3], and (2) express multiple cardiac ion channels, thus generating a typical human action potential (AP) [2, 3]. Unfortunately, hiPSC-CMs are structurally and functionally immature, resembling fetal CMs [4]. This immature phenotype of hiPSC-CMs affects their usability. Therefore, there is an urgent need to mature hiPSC-CMs.

HiPSC-CMs poorly recapitulate electrophysiological properties of adult human cardiomyocytes (CMs). In adult CMs, three K^+ currents tightly regulate the configuration of AP: the rapid (I_{Kr}) and slow (I_{Ks}) delayed rectifier K^+ currents and the inward rectifier current (I_{K1}). Highly expressed I_{K1}, I_{Kr} and I_{Ks} ensure stable and constant AP signaling in adult CMs. The hyperpolarization-activated, “funny” current (I_f) is a mixed Na^+ and K^+ inward current activating at voltages below −40/−45 mV [5]. If can trigger spontaneous APs and generate pacemaking activity [5, 6]. In the adult heart, I_f only exists in pacemaker cells dedicated to generating spontaneous activity and modulating sympathetic acceleration capacities of the heart rate [5]. Unfortunately, hiPSC-CMs typically have a large amount of I_f but a low amount or near-complete absence of I_{K1}, I_{Kr} and I_{Ks} [7]. These features reduce the utility of hiPSC-CMs for disease modeling and drug screening [8]. Therefore, increased I_{K1}, I_{Kr} and I_{Ks} and reduced I_f would be crucial to improving the fidelity of hiPSC-CMs as human CM models.

How can we improve the electrophysiological maturation of hiPSC-CMs? In humans, fetal CMs require around 280 days to reach a neonatal phenotype. The heart’s electrophysiological maturation process involves upregulating I_{K1}, I_{Kr}, and I_{Ks}, and reducing I_f in ventricle [9, 10]. However, hiPSC-CMs are normally generated in the dish within 30 days [1], and they resemble the first trimester of the human fetal heart (gestational weeks 7-10) [4]. Unsurprisingly, day 30^{th} hiPSC-CMs typically exhibit low I_{K1}, I_{Kr}, and I_{Ks} but high I_f. Hence, one logical way to achieve a more mature phenotype is to increase the culture time of hiPSC-CMs. Sartiani et al. [11] demonstrated that culture durations greater than 3-months increased I_{K1} and I_{Kr} and reduced I_f in human embryonic stem cell derived-CMs (hESC-CMs). Wang et al. [12] also found that culturing more than 80 days can shorten APD and increase CV in hESC-CM monolayers. Recently, Feyen et al. [13]

used physiological levels of glucose and calcium and a mixture of fatty acids to culture hiPSC-CMs over 21 to 35 days, which significantly increased I_{K1}. Therefore, the critical challenge is how to increase I_{K1}, I_{Kr}, and I_{Ks} and reduce I_f in hiPSC-CMs rapidly and consistently.

More evidence suggests the significant roles of triiodothyronine (T3) and dexamethasone (Dex) in the CM maturation. Several reports have documented that T3 and Dex can upregulate transcription levels for K^+ channels in CMs, respectively [14–17]. Dex has also been reported to facilitate the K^+ channel trafficking via serine/threonine protein kinase (SGK) and enhance their membrane expression [18–20]. Our previous study showed the combined T3 and Dex can promote the functional T-tubule development in hiPSC-CMs [21]. However, it was unclear about the effects of T3+Dex on the K^+-channel expression in hiPSC-CMs. In this study, we treated hiPSC-CMs with a combination of T3+Dex for 14 days. We found that T3+Dex treatment changed the gene expression of K^+ channels, increased I_{K1}, I_{Kr}, and I_{Ks}, and reduced I_f, thereby enhancing the electrophysiological maturation of hiPSC-CMs.

2. Methods

HiPSC lines were approved by Vanderbilt University Medical Center Institutional Review Board.

2.1 HiPSC maintenance and cardiac differentiation

All cultures were kept in a humidified incubator at 37°C and maintained with a 5% CO_2 atmosphere. HiPSC lines were cultured as described previously [2, 22]. Briefly, hiPSCs were cultured in a home-made E8 medium [23]. Cardiac differentiation was induced from monolayers using small molecules CHIR99021 (Selleck Chemicals) and IWR-1 (Sigma) [2, 21]. On day 15, hiPSC-CMs were dissociated and replated on Matrigel-coated 6-well plated. HiPSC-CMs were treated with 100 nmol/L triiodothyronine (T3, Sigma) and 1 μmol/L Dexamethasone (Dex, Cayman), or vehicle from day 16 to 30.

2.2 Optical mapping

On day 15, 0.9-1.1×10^6 hiPSC-CMs were seeded as a circular (diameter: 0.5 mm) hiPSC-derived cardiomyocyte cell sheets (hiPSC-CCSs) on Matrigel-coated 35mm dishes. Day 16^{th} hiPSC-CCSs were treated with vehicle or T3+Dex for 14 days. On day 30^{th}, the culture medium was switched to a regular medium, and the cultures were optically mapped 2 days later. Mapping experiments were carried out at 37°C humidified with CO_2, as described in [24]. Briefly, hiPSC-CCSs were loaded with FluoVolt (F10488, Molecular Probes) using the manufacturer protocol. HiPSC-CCSs were stimulated using a costume-made platinum electrode connected to a stimulus isolation unit (SIU-102, Warner Instrument). The mapping of hiPSC-CCSs was carried out using a high-speed EM-CCD camera (Evolve 512Delta, Photometrics) mounted on a fluorescent microscope (MVX10, Olympus). The tissues were excited using 475nm LED (Excelitas Technologies), the emission was passed through a 495 nm LP dichroic mirror and filtered using a 525/50nm B.P. filter. Videos were acquired

and analyzed using OMProCCD [25], a custom-designed software kindly provided by Prof. Bum-Rak (Brown University) to derive activation and APD maps.

2.3 RNA sequencing

Total RNA was extracted from vehicle- or T3+Dex-treated hiPSC-CMs with RNeasy Mini Kit (QIAGEN) followed by DNase treatment. Each demultiplexed sample was analyzed using FASTqc for overall quality, followed by trimming low quality or biased reads using seqtk (https://github.com/lh3/seqtk). Transcript abundances were calculated using Salmon 0.8.2, the recently developed psuedomapping algorithm for rapid RNAseq analyses [26]. Reads were mapped to the GRCh38.p12 build of the human genome using the parameters-k 31, -seqBias, -gcBias, -posBias. Differential expression was determined using the DESEQ2 R package using default parameters [27]. Gene Enrichment Analyses were performed using the GeneAnalytics Suite, which used the binomial distribution-based enrichment analysis and reported Benjamini-Hochberg-adjusted p values [28].

2.4 Spontaneous beating rate of single cells

On day 30, vehicle or T3+Dex-treated hiPSC-CMs were dissociated and cultured on Matrigel Mattress for an additional 3 to 5 days before the experiment [1]. The Matrigel Mattress method provided a physiological load (5-7kPa) and generated the rod-like shape of hiPSC-CMs. The spontaneous beating rate was counted on the rod-shaped hiPSC-CMs under a bright-light microscope at room temperature.

2.5 Single-cell Electrophysiology

APs and I_{Na} were recorded from single hiPSC-CMs cultured on Matrigel Mattress. I_{K1}, I_f, I_{Kr}, and I_{Ks} were recorded from single hiPSC-CMs cultured on 1:200 diluted Matrigel. The pipettes were prepared from 1.5-mm thin-walled borosilicate glass capillaries using a micropipette puller and had resistances in the range of 3-5 MΩ. Current and voltage clamp were perfomed by using Axonpatch 200B, Digidata 1322A and pClamp 10.7 software (Axon Instrument) for data amplification and acquisition. Cell capacitances were comparable between vehicle- and T3+Dex-treated hiPSC-CMs.

I_{Kr} and I_{Ks} were recorded in Tyrode solution with 10 μmol/L nifedipine at 35-37°C. To record I_{Kr}, the membrane potential was held at −80 mV followed by −40 mV, and currents were elicited by 1-s test pulses from 20 to −40 mV at 10-mV decrement. I_{Kr} were isolated as 0.5 μmol/L E-4031-sensitive currents. To record I_{Ks}, the membrane potential was held at −80 mV followed by −40 mV, and currents were elicited by 4-s test pulses from 40 to −40 mV at 20-mV decrement, I_{Ks} were isolated as 0.5 μmol/L HMR1556-sensitive currents under the continuous perfusion of E-4031 (0.5 μmol/L).

I_{K1} and I_f were recorded in modified Tyrode solution with 0.2 mmol/L $CdCl_2$ at room temperature. From the holding potential of −40 mV, I_{K1} was elicited by 500-ms test pulses from −120 to 0 mV at 10-mV increments, I_{K1} were defined as 0.5 mmol/L Ba^{2+}-sensitive currents. To measure I_f currents, the membrane potential was held at −40 mV, and I_f was elicited by 2-s test pulses from −120 to −50 mV at 10-mV increments. I_f were defined as 0.05 mmol/L Ba^{2+}-insensitive and 5 mmol/L Cs^+-sensitive currents.

I_{Na} were measured using K^+-free external solution with 1 μpmol/L nisoldipine and 200 μmol/L $NiCl_2$ at room temperature as described in [1]. Briefly, I_{Na} was measured by applying 40 ms test pulse between −80 and 60 mV at 10 mV increments from the holding potential of −120 mV. Steady-state inactivation was measured by varying the hold potential from −140 to −20 mV, followed by a 40-ms test pulse to −20 mV.

APs were measured at room temperature with the rupture patch-clamp technique as described in [2]. Briefly, a 2-ms current pulse at 20% above threhold was provided to evoke APs at a cycle length of 2 s (0.5 Hz).

Modified Tyrode solution was composed of (mmol/L): 120 NaCl, 20 KCl, 10 HEPES, 10 Glucose, 2 $CaCl_2$ and 1 $MgCl_2$, pH adjusted to 7.4 with NaOH. Tyrode solution contained the following (mmol/L): 137 NaCl, 5.4 KCl, 10 HEPES, 10 Glucose, 1 $MgCl_2$, 1.8 $CaCl_2$, pH adjusted to 7.4 with NaOH. K^+-free external solution contained (mmol/L): 5 NaCl, 135 CsCl, 10 HEPES, 10 Glucose, 1 $MgCl_2$, $CaCl_2$; pH adjusted to 7.4 with CsOH. For I_{Kr} and I_{Ks} recordings, the pipette solution contained (mmol/L): 150 KCl, 5 NaCl, 2 $CaCl_2$, 5 EGTA, 5 HEPES, 5 MgATP, pH was adjusted to 7.2 by KOH. For I_{K1} and I_f recordings, the pipette solution contained (mmol/L): 100 KCl, 10 NaCl, 14 EGTA, 10 HEPES, 5 MgATP, 1 $CaCl_2$; pH adjusted to 7.2 with KOH. For I_{Na} recording, the pipette solution contained (mmol/L): 5 NaCl, 135 CsCl, 5 EGTA, 10 HEPES, 5 MgATP, 2 $CaCl_2$; pH adjusted to 7.2 with CsOH. For the AP measurement, the pipette solution contained (mmol/L): 110 KCl, 5 NaCl, 5 Mg-ATP, 10 HEPES, 5 Phosphocreatine, pH adjusted to 7.2 with KOH. Stock solutions of E4031 (500 μmol/L, TOCRIS) and $NiCl_2$ (1 mol/L, Sigma) was prepared in distilled water. Nisoldipine (50 mmol/L, Sigma), Nifedipine (50 mmol/L, Sigma) and HMR1556 (500 μmol/L, TOCRIS) were dissolved in DMSO. All stock solutions were freshly diluted in recording solution before use.

2.6 Western blot

Day 30th vehicle- and T3+Dex-treated hiPSC-CMs were lysed with RIPA buffer supplemented with PhosSTOP and EDTA-free protease inhibitor cocktail (Sigma). All lysates were centrifuged at 13,000 rpm for 20 min at 4°C. Protein was quantified using Bradford Protein assay (Bio-rad). 22.5 μg of protein lysates were resolved on 4-20% Tris Glycine gel in Tris-Glycine-SDS buffer (Bio-rad) and transferred onto nitrocellulose membranes for immunoblotting. Membrane was blocked in TBST (Tris-buffered saline, 0.1% Tween 20) with 5% milk for 1 hour. Membranes were incubated with primary antibody anti-connexin 43 (1: 2,000, Abcam, ab217676) overnight at 4°C, and then in secorday antibody (1:2,000, Cell signal, #7074) for 1 hour. Membranes were incubated with ECL substrate (Thermo) for 5 min and developed on Bio-rad ChemiDoc MP imaging system (Bio-rad). After imaging, membranes were stripped with Restore Western Blot Stripping Buffer (Thermo), and stained with α-actinin (primary antibody: 1: 2,000, Sigma, EA-53; secondary antibody: 1:2,500, Invitrogen, 31430). Connexin 43 band intensities were quantified and normalized to α-actinin using Image J.

2.7 Statistical analysis

Data were presented as mean ± SEM. The electrophysiological data were analyzed using Clampfit 10.5, and curve fitting was performed by GraphPad Prism 8 (GraphPad Software). Statistical differences were evaluated using unpaired two tailed t-test or two-way ANOVA followed by Sidak's multiple comparisons test or Dunnett's multiple comparisons test. $p < 0.05$ was considered as statistical significance.

3. Results

3.1 Conduction velocity and action potential duration in hiPSC-CM cell sheets

We used optical mapping to measure CV and APD at 80% repolarization (APD_{80}) in FluVolt-loaded hiPSC-derived cardiomyocyte cell sheets (hiPSC-CCSs) at different electrically-stimulated pacing-cycle lengths (400, 500, 666, 800, and 1000 ms). Fig. 1A shows examples of optical AP signals derived from vehicle- and T3+Dex-treated hiPSC-CCSs when paced at a cycle length of 1000 ms. Figs. 1B and C depict the resulting APD_{80} and CV restitution curves obtained from the vehicle- and T3+Dex-treated hiPSC-CCSs. Note the characteristic shortening of APD_{80} and slowing of CV as pacing frequency increases. Importantly, at each pacing cycle length, T3+Dex-treated hiPSC-CCSs exhibited significantly faster CV and shorter APD_{80} values than the vehicle-treated specimens, demonstrating the strong impact of the combined T3+Dex treatment.

Next, we studied the does-dependent effect of $BaCl_2$ on APD_{80} and conduction velocity when paced at a cycle length of 1000 ms. The results showed that 10 and 100 μM $BaCl_2$ significantly prolonged APD80 in T3+Dex-treated hiPSC-CCSs (Fig. 1C). 100 μM $BaCl_2$ slowed conduction velocity in T3+Dex-treated hiPSC-CCSs (Fig. 1D). Vehicle-treated hiPSC-CCSs were completely insensitive to $BaCl_2$ treatment.

3.2 Spontaneous activity and action potential characteristics in single hiPSC-CMs

We next examined the effect of T3+Dex on the spontaneous beating rate (beats per min; bpm) and AP properties in single hiPSC-CMs. As shown in Fig. 2A, T3+Dex-treated hiPSC-CMs had slower spontaneous beating rates than vehicle-treated cells (vehicle: 17.48 ± 0.84 vs. T3+Dex: 11.96 ± 0.82 bpm, $p = 0.000005$). Fig. 2B displayed a sample tracing of APs recorded in vehicle- and T3+Dex-treated hiPSC-CMs at 0.5-Hz pacing. The measured AP parameters derived from the recordings made from vehicle- and T3+Dex-treated hiPSC-CMs were summarized in Table 1. These results showed that T3+Dex-treated hiPSC-CMs had a significantly more hyperpolarized resting membrane potential (RMP) than the vehicle-treated cells. Moreover, T3+Dex-treated hiPSC-CMs had faster maximal upstroke velocity (V_{max}), larger AP amplitude, and a shorter APD at 50% and 90% repolarization (APD_{50} and APD_{90}) than the vehicle. The overshoot of the AP (between 0 mV and the peak of AP) was comparable between vehicle- and T3+Dex-treated hiPSC-CMs.

3.3 Potassium channel-related gene expression

To understand how T3+Dex treatment change the electrophysiological properties of hiPSC-CMs, we compared the gene expression profiles between vehicle- and T3+Dex-treated hiPSC-CMs. In the RNA-sequencing dataset, T3+Dex-treated hiPSC-CMs showed 7551

significant differentially expressed genes (adjusted $p < 0.05$). Given the critical role of K^+ channels in determining cardiac automaticity and AP properties, we then identified 95 genes encoding for K^+ channels, of which 37 genes were significantly changed in T3+Dex-treated hiPSC-CMs (Fig. 3A). As shown in Fig. 3B, *KCNJ2* and *KCNJ12* (contributing to I_{K1}), *KCNH2* and *KCNE2* (contributing to I_{Kr}), *KCNQ1* (contributing to I_{Ks}) were significantly increased in T3+Dex-treated hiPSC-CMs; but *HCN4* (contributing to I_f) was decreased. But *SCN5A* (contributing to I_{Na}) was comparable between vehicle- and T3+Dex-treated hiPSC-CMs. To determine whether gene expression was correlated with cellular electrophysiological properties, we next used patch-clamp to measure I_{K1}, I_{Kr}, I_{Ks}, I_f, and I_{Na} in vehicle- and T3+Dex-treated hiPSC-CMs.

3.4 Inward rectifier current (I_{K1}) and funny current (I_f)

In vehicle-treated hiPSC-CMs, I_{K1} was very small and difficult to record when 5.4 mmol/L K^+ was present in the extracellular solution. Hence, we increased the extracellular K^+ concentration to 20 mmol/L to evoke a larger I_{K1}. Fig. 4A and B show typical traces of I_{K1} in the vehicle- and T3+Dex-treated hiPSC-CMs. The resulting plot of the current-voltage (I-V) relationship (Fig. 4C) shows that the average peak current density (at −120 mV) was approximately 4-fold larger in T3+Dex-treated hiPSC-CMs compared to vehicle-treated cells (vehicle −4.62 ± 0.59 vs. T3+Dex −18.79 ± 1.98 pA/pF, $p = 0.0003$).

Fig. 5A and B illustrate typical I_f traces in vehicle- and T3+Dex-treated hiPSC-CMs. I_f density at −120 mV was signficantlysmaller in T3+Dex-treated hiPSC-CMs compared to vehicle (vehicle: −12.20 ± 2.15 vs. T3+Dex: −6.98 ± 0.89 pA/pF, $p = 0.001$, Fig. 5C). We next normalized the If current density at each voltage step to the maximal current density at −120 mV and then generated the I_f activation curve. As shown in Fig. 5D, when fitting with a Boltzmann function, the half maximum activation voltage ($V_{1/2}$) and slope factor (k values) for If in vehicle-treated cells were −101.25 ± 2.21 mV and −12.76 ±1.00, respectively. The $V_{1/2}$ and k values in the T3+Dex-treated hiPSC-CMs were −101.92 ± 2.16 mV and −15.08 ± 1.27.

3.5 Delayed rectifier currents (I_{Kr} and I_{Ks})

We used pharmacological dissection to identify, isolate, and quantify I_{Kr} and I_{Ks}. Figs. 6A and B show representative I_{Kr} traces in vehicle- and T3+Dex-treated hiPSC-CMs. The I-V plot (Fig. 6C) shows that I_{Kr} was significantly larger in T3+Dex-treated hiPSC-CMs compared to the vehicle (peak at −10 mV, vehicle: 0.48 ± 0.05 vs. T3+Dex: 0.93 ± 0.14 pA/pF, $p = 0.00005$). T3+Dex-treated hiPSC-CMs also exhibited significantly larger peak tail current density than the vehicle-control cells (at 20 mV, vehicle: 0.81 ± 0.07 vs. T3+Dex: 1.35 ± 0.19 pA/pF, $p = 0.002$). After fitting with a Boltzmann function, $V_{1/2}$ and k values for I_{Kr} were −18.83 ± 1.29 mV and 7.44 ± 0.62 in the vehicle-treated hiPSC-CMs and −22.85 ± 1.26 mV and 7.03 ± 0.46 in T3+Dex-treated hiPSC-CMs (Fig. 6D).

Figs. 7A and B show representative I_{Ks} traces in vehicle- and T3+Dex-treated hiPSC-CMs. The I-V plot (Fig. 7C) showed that T3+Dex-treated hiPSC-CMs had signficantly larger I_{Ks} compared vehicle (peak current at 40 mV, vehicle: 0.38 ± 0.06 vs. T3+Dex: 0.72 ±0.17 pA/pF, $p = 0.004$).

3.6 Sodium current (I_{Na})

Compared to vehicle, T3+Dex treatment significantly increased conduction velocity (Fig. 1E) and the V_{max} of the AP upstroke (Table 1). Both parameters are related to the available Na^+ conductance [29, 30]. Even though T3+Dex treatment did not significantly change SCN5A expression in hiPSC-CMs (online Fig. 2A), we directly measured I_{Na} in vehicle- and T3+Dex-treated hiPSC-CMs. Fig. 8A and B present representative traces of I_{Na} in vehicle-and T3+Dex-treated hiPSC-CMs. The I-V plot (Fig. 8C) showed that I_{Na} was more than 4-fold increased in T3+Dex-treated hiPSC-CMs compared to vehicle (at −30 mV, vehicle −9.8 ± 1.86 vs. T3+Dex −44.9 ±7.10 pF/pA, $p = 0.003$). After fitting with a Boltzmann function, $V_{1/2}$ and k values for I_{Na} were −81.83 mV and −5.82 in the vehicle and −83.39 mV and −6.27 in T3+Dex-treated hiPSC-CMs (Fig. 8D).

4. Discussion

This study reports the effects of T3 and Dex on the electrophysiological properties of hiPSC-CMs. We found that T3+Dex treatment: (1) increased CV and shortened APD_{80} in hiPSC-CCs; (2) slowed spontaneous beating rate of single hiPSC-CMs; (3) led to a more hyperpolarized RMP, faster V_{max}, and shorter APD in single hiPSC-CMs; (4) changed the expression of genes encoding for K^+ channels; (5) increased I_{Na}, I_{K1}, I_{Kr}, and I_{Ks}, and reduced I_f in hiPSC-CMs.

How does T3+Dex treatment alter the expression of potassium channels in hiPSC-CMs?

Previous studies have shown that T3 and Dex can regulate transcription of K^+ channel genes via activating their nuclear receptors (thyroid hormone receptors (TRs) and glucocorticoid receptor (GR), respectively) [15, 19, 31–34]. Once T3 and Dex activate their nuclear receptors, TRs and GR act as transcription factors that bind to their cognate response elements in the promoters of target genes and regulate transcriptional activity. In addition, Dex has been shown to enhance the K^+ channel trafficking by SGK [12, 15–17]. Our RNAseq data showed that T3+Dex treatment significantly increases the expression of *THRA, THRB, NR3C1* (encoded for TRα, TRβ and GR, respectively), *SGK1* and *SGK2* (online Fig. 1). This result is consistent with the observed increase in the transcription levels for I_{K1}, I_{Kr}, and I_{Ks}, and the reduced transcription for I_f in hiPSC-CMs. Our current clamp results confirmed corresponding changes in channel function, with I_{K1}, I_{Kr}, and I_{Ks} increased, and I_f reduced in T3+Dex-treated hiPSC-CMs.

I_{Na}, I_{K1}, and I_f of T3+Dex-treated hiPSC-CMs

I_{Na} provides a rapid depolarizing current during the upstroke of AP, which is an important determinant of the conduction velocity and APD [35]. In this study, T3+Dex treatment significantly increased I_{Na} in hiPSC-CMs. This increase in I_{Na} contributes to the faster V_{max} in APs (Table 1) and the faster CV (Fig. 1C). In addition, I_{K1} also plays a key role in modulating cardiac excitability and CV [36, 37]. I_{K1} serves as the primary current to hyperpolarize the membrane potential [38–41]. Due to a low I_{K1}, vehicle-treated hiPSC-CMs had a relatively depolarized RMP (−65.0 mV). After T3+Dex treatment, I_{K1} displayed a 5-fold increase, giving rise to a more negative RMP (−72.0 mV) in hiPSC-CMs (Table 1). By setting a more negative RMP, an increase in I_{K1} enhaces the availability of

sodium channels during sustained reentry, thereby regulating cardiac excitability and CV. This may explain why inhibition of I_{K1} with $BaCl_2$ slowed the CV of T3+Dex-treated hiPSC-CCSs (Fig. 1E). In addition to I_{K1}, cell-cell coupling via gap junctions (formed by connexin 43 channels) is another important determinant of CV [42, 43]. Consistent with this idea, T3+Dex treatment significantly increased the transcription and protein expression of connexin 43 (online Fig. 2), likely also contributing to a faster CV in hiPSC-CCSs (Fig. 1E). I_{K1} is also important for the late repolarization of APs [40]. Accordingly, inhibtion of I_{K1} by $BaCl_2$ significantly prolonged APD in T3+Dex-treated hiPSC-CCSs (Fig. 1D).

Unlike the human ventricle, hiPSC-CMs possess abundant I_f that can spontaneously fire APs and generate pacemaking activity [5]. Vehicle-treated hiPSC-CMs had a faster pacemaking activity caused by higher I_f. After T3+Dex treatment, I_f was significantly decreased in hiPSC-CMs and I_{K1} became the dominant current during diastolic depolarization phase, which led to a 50% reduction in the pacemaking activity (Fig. 2A).

I_{Kr}, I_{Ks}, and action potential of T3+Dex-treated hiPSC-CMs

Previous work had documented that I_{Kr} as the dominant repolarizing K^+ current in hiPSC-CMs, whereas I_{Ks} is much lower than I_{Kr} [7]. Consistent with the previous work, we also found that I_{Kr} was present in all vehicle-treated hiPSC-CMs, but I_{Ks} was only found in a small fraction (25%) of vehicle-treated hiPSC-CMs. T3+Dex treatment significantly increased both I_{Kr} and I_{Ks}, and I_{Ks} were present in 76% of cells. Did the increased I_{Kr} and I_{Ks} contribute to the shorter APD of T3+Dex-treated hiPSC-CMs (Fig. 2B)? It is generally accepted that I_{Kr} plays a critical role in the repolarization process. In hiPSC-CMs, blockade of I_{Kr} prolongs APD [44, 45], and I_{Kr} activation shortens APD [46], which is consistent with findings in the human heart [47, 48]. For I_{Ks}, previous studies have shown that its contribution to AP repolarization is limited to the presence of β-adrenergic stimulation or in the setting of reduced repolarization reserve (i.e., I_{Kr} blockage) [7, 44]. Ma et al. reported that suppression of I_{Ks} by 3R4S-chromanol 293B had minial effects on APD in hiPSC-CMs [7]. On the other hand, KCNQ1 mutations, which severely reduce I_{Ks}, results in APD prolongation in hiPSC-CMs without the activation of β-adrenergic receptor or the reduced repolarization reserve [46]. Therefore, it is likely that increased I_{K1}, I_{Kr}, and I_{Ks}, all contributed to the shorter APD of T3+Dex-treated hiPSC-CMs.

In this study, we observed that APDs were longer in single hiPSC-CMs than in 2D cultured hiPSC-CCSs. A number of factors likely contributed to the longer APD of single cells. Compared to hiPSC-CCSs, single-cell APs were recorded at lower temperature (20 vs 37°C) and slower pacing frequency (0.5 vs 1 Hz). Faster pacing frequency and higher temperature are known to shorten APDs [49, 50]. Furthermore, in 2D culture, hiPSC-CCSs were coupled to adjacent CMs and non-myocytes, which also leads to a shorter APD [43, 51, 52].

Compared with the human ventricle, where the reported RMP varies from −80 mV to −86 mV and APD_{90} from 213 to 351 ms [53, 54], T3+Dex-treated hiPSC-CMs had a more depolarized RMP and more prolonged APD_{90}. It indicates that even after treatment with T3+Dex hiPSC-CMs are still less mature than adult human CMs.

5. Conclusion

T3+Dex treatment increased CV and shortened APD in hiPSC-CCSs. Moreover, in single hiPSC-CMs, T3+Dex treatment slowed spontaneous beating rates and led to a more hyperpolarized RMP, faster V_{max}, and shorter APD. These changes were mediated by increasing I_{Na}, I_{K1}, I_{Kr}, and I_{Ks}, and reduced I_f in T3+Dex-treated hiPSC-CMs. Thus, our results demonstrate that T3+Dex treatment is a practical approach to improve electrophysiological maturation of hiPSC-CMs within 30 days of cardiac differentiation.

Supplementary Material

Refer to Web version on PubMed Central for supplementary material.

Disclosure of funding

The work was supported by Leducq Foundation 18CVD05 (to B.C.K. and L.G.), by the National Institutes of Health NHLBI R35 HL144980 (to B.C.K.), by American Heart Association 19POST34380182 (to L.L.W.), by Heart Rhythm Society Clinical Research Award in Honor of Mark Josephson and Hein Wellens (to Y.W.), by National Institutes of Health NHLBI T32 HL007411-39 (to J.S.).

There are no relationships with the industry. The authors declare no financial conflict of interest.

Abbreviations

hiPSC
Human-induced pluripotent stem cell

CM
Cardiomyocyte

hiPSC-CCS
hiPSC-derived cardiomyocyte cell sheet

T3
Triiodothyronine

Dex
Dexamethasone

CV
Conduction velocity

APD_{50}, APD_{80} and APD_{90}
Action potential duration at 50, 80 and 90% repolarization

RMP
Resting membrane potential

V_{max}
Maximal upstroke velocity

I_{Na}
Sodium current

I_{K1}
Inward rectifier potassium current

I_f
Hyperpolarization-activated (“funny”) current

I_{Kr}
Rapid activating delayed rectifier potassium current

I_{Ks}
Slow activating delayed rectifier potassium current

Reference

[1]. Feaster TK, Cadar AG, Wang L, Williams CH, Chun YW, Hempel JE, et al. Matrigel Mattress: A Method for the Generation of Single Contracting Human-Induced Pluripotent Stem Cell-Derived Cardiomyocytes. Circ Res 2015;117:995–1000. [PubMed: 26429802]

[2]. Wang L, Kim K, Parikh S, Cadar AG, Bersell KR, He H, et al. Hypertrophic cardiomyopathy-linked mutation in troponin T causes myofibrillar disarray and pro-arrhythmic action potential changes in human iPSC cardiomyocytes. J Mol Cell Cardiol 2018;114:320–7. [PubMed: 29217433]

[3]. Hwang HS, Kryshtal DO, Feaster TK, Sanchez-Freire V, Zhang J, Kamp TJ, et al. Comparable calcium handling of human iPSC-derived cardiomyocytes generated by multiple laboratories. J Mol Cell Cardiol 2015;85:79–88. [PubMed: 25982839]

[4]. van den Berg CW, Okawa S, Chuva de Sousa Lopes SM, van Iperen L, Passier R, Braam SR, et al. Transcriptome of human foetal heart compared with cardiomyocytes from pluripotent stem cells. Development 2015;142:3231–8. [PubMed: 26209647]

[5]. DiFrancesco D The Role of the Funny Current in Pacemaker Activity. Circ Res 2010;106:434–46. [PubMed: 20167941]

[6]. Chan YC, Siu CW, Lau YM, Lau CP, Li RA, Tse HF. Synergistic effects of inward rectifier (I) and pacemaker (I) currents on the induction of bioengineered cardiac automaticity. J Cardiovasc Electrophysiol 2009;20:1048–54. [PubMed: 19460073]

[7]. Ma J, Guo L, Fiene SJ, Anson BD, Thomson JA, Kamp TJ, et al. High purity human-induced pluripotent stem cell-derived cardiomyocytes: electrophysiological properties of action potentials and ionic currents. Am J Physiol Heart Circ Physiol 2011;301:H2006–17. [PubMed: 21890694]

[8]. Hoekstra M, Mummery CL, Wilde AA, Bezzina CR, Verkerk AO. Induced pluripotent stem cell derived cardiomyocytes as models for cardiac arrhythmias. Front Physiol 2012;3:346. [PubMed: 23015789]

[9]. Harrell MD, Harbi S, Hoffman JF, Zavadil J, Coetzee WA. Large-scale Analysis of Ion Channel Gene Expression in the Mouse Heart During Perinatal Development. Physiol Genomics 2007;28:273–83. [PubMed: 16985003]

[10]. Davies MP, An RH, Doevendans P, Kubalak S, Chien KR, Kass RS. Developmental Changes in Ionic Channel Activity in the Embryonic Murine Heart. Circ Res 1996;78:15–25. [PubMed: 8603498]

[11]. Sartiani L, Bettiol E, Stillitano F, Mugelli A, Cerbai E, Jaconi ME. Developmental changes in cardiomyocytes differentiated from human embryonic stem cells: a molecular and electrophysiological approach. Stem Cells 2007;25:1136–44. [PubMed: 17255522]

[12]. Wang Y, Zhu R, Tung L. Contribution of Potassium Channels to Action Potential Repolarization of Human Embryonic Stem Cell-Derived Cardiomyocytes. Br J Pharmacol 2019;176:2780–94. [PubMed: 31074016]

[13]. Feyen DAM, McKeithan WL, Bruyneel AAN, Spiering S, Hormann L, Ulmer B, et al. Metabolic Maturation Media Improve Physiological Function of Human iPSC-Derived Cardiomyocytes. Cell Rep 2020;32:107925. [PubMed: 32697997]

[14]. Nishiyama A, Kambe F, Kamiya K, Yamaguchi S, Murata Y, Seo H, et al. Effects of thyroid and glucocorticoid hormones on Kv1.5 potassium channel gene expression in the rat left ventricle. Biochem Biophys Res Commun 1997;237:521–6. [PubMed: 9299396]

[15]. Watanabe H, Ma M, Washizuka T, Komura S, Yoshida T, Hosaka Y, et al. Thyroid hormone regulates mRNA expression and currents of ion channels in rat atrium. Biochem Biophys Res Commun 2003;308:439–44. [PubMed: 12914768]

[16]. Takimoto K, Fomina AF, Gealy R, Trimmer JS, Levitan ES. Dexamethasone rapidly induces Kv1.5 K+ channel gene transcription and expression in clonal pituitary cells. Neuron 1993;11:359–69. [PubMed: 8352944]

[17]. Levitan ES, Hemmick LM, Birnberg NC, Kaczmarek LK. Dexamethasone Increases Potassium Channel Messenger RNA and Activity in Clonal Pituitary Cells. Mol Endocrinol 1991;5:1903–8. [PubMed: 1791837]

[18]. Seebohm G, Strutz-Seebohm N, Ursu ON, Preisig-Muller R, Zuzarte M, Hill EV, et al. Altered stress stimulation of inward rectifier potassium channels in Andersen-Tawil syndrome. FASEB J 2012;26:513–22. [PubMed: 22002906]

[19]. Lamothe SM, Zhang S. The serum- and glucocorticoid-inducible kinases SGK1 and SGK3 regulate hERG channel expression via ubiquitin ligase Nedd4-2 and GTPase Rab11. J Biol Chem 2013;288:15075–84. [PubMed: 23589291]

[20]. Seebohm G, Strutz-Seebohm N, Birkin R, Dell G, Bucci C, Spinosa MR, et al. Regulation of endocytic recycling of KCNQ1/KCNE1 potassium channels. Circ Res 2007;100:686–92. [PubMed: 17293474]

[21]. Parikh SS, Blackwell DJ, Gomez-Hurtado N, Frisk M, Wang L, Kim K, et al. Thyroid and Glucocorticoid Hormones Promote Functional T-tubule Development in Human-Induced Pluripotent Stem Cell Derived Cardiomyocytes. Circ Res 2017;121:1323–30. [PubMed: 28974554]

[22]. Chavali NV, Kryshtal DO, Parikh SS, Wang L, Glazer AM, Blackwell DJ, et al. Patient-independent human induced pluripotent stem cell model: A new tool for rapid determination of genetic variant pathogenicity in long QT syndrome. Heart Rhythm 2019;16:1686–95. [PubMed: 31004778]

[23]. Burridge PW, Matsa E, Shukla P, Lin ZC, Churko JM, Ebert AD, et al. Chemically defined generation of human cardiomyocytes. Nat Methods 2014;11:855–60. [PubMed: 24930130]

[24]. Shaheen N, Shiti A, Huber I, Shinnawi R, Arbel G, Gepstein A, et al. Human Induced Pluripotent Stem Cell-Derived Cardiac Cell Sheets Expressing Genetically Encoded Voltage Indicator for Pharmacological and Arrhythmia Studies. Stem Cell Reports 2018;10:1879–94. [PubMed: 29754959]

[25]. Huang XD, Kim TY, Koren G, Choi BR, Qu ZL. Spontaneous Initiation of Premature Ventricular Complexes and Arrhythmias in Type 2 Long QT Syndrome. Am J Physiol Heart Circ Physiol 2016;311:H1470–84. [PubMed: 27765749]

[26]. Patro R, Duggal G, Love MI, Irizarry RA, Kingsford C. Salmon provides fast and bias-aware quantification of transcript expression. Nat Methods 2017;14:417–9. [PubMed: 28263959]

[27]. Love MI, Huber W, Anders S. Moderated estimation of fold change and dispersion for RNA-seq data with DESeq2. Genome Biol 2014;15:550. [PubMed: 25516281]

[28]. Ben-Ari Fuchs S, Lieder I, Stelzer G, Mazor Y, Buzhor E, Kaplan S, et al. GeneAnalytics: An Integrative Gene Set Analysis Tool for Next Generation Sequencing, RNAseq and Microarray Data. OMICS 2016;20:139–51. [PubMed: 26983021]

[29]. O'Shea C, Pavlovic D, Rajpoot K, Winter J. Examination of the Effects of Conduction Slowing on the Upstroke of Optically Recorded Action Potentials. Front Physiol 2019;10:1295. [PubMed: 31681008]

[30]. Kodama I, Toyama J, Yamada K. Competitive inhibition of cardiac sodium channels by aprindine and lidocaine studied using a maximum upstroke velocity of action potential in guinea pig ventricular muscles. J Pharmacol Exp Ther 1987;241:1065–71. [PubMed: 2439681]

[31]. Gloss B, Trost S, Bluhm W, Swanson E, Clark R, Winkfein R, et al. Cardiac ion channel expression and contractile function in mice with deletion of thyroid hormone receptor alpha or beta. Endocrinology 2001;142:544–50. [PubMed: 11159823]

[32]. Le Bouter S, Demolombe S, Chambellan A, Bellocq C, Aimond F, Toumaniantz G, et al. Microarray analysis reveals complex remodeling of cardiac ion channel expression with altered thyroid status: relation to cellular and integrated electrophysiology. Circ Res 2003;92:234–42. [PubMed: 12574152]

[33]. Levitan ES, Hershman KM, Sherman TG, Takimoto K. Dexamethasone and stress upregulate Kv1.5 K+ channel gene expression in rat ventricular myocytes. Neuropharmacology 1996;35:1001–6. [PubMed: 8938730]

[34]. Ballou LM, Lin RZ, Cohen IS. Control of cardiac repolarization by phosphoinositide 3-kinase signaling to ion channels. Circ Res 2015;116:127–37. [PubMed: 25552692]

[35]. Fozzard HA, Hanck DA. Structure and function of voltage-dependent sodium channels: comparison of brain II and cardiac isoforms. Physiol Rev 1996;76:887–926. [PubMed: 8757791]

[36]. Milstein ML, Musa H, Balbuena DP, Anumonwo JM, Auerbach DS, Furspan PB, et al. Dynamic reciprocity of sodium and potassium channel expression in a macromolecular complex controls cardiac excitability and arrhythmia. Proc Natl Acad Sci U S A 2012;109:E2134–43. [PubMed: 22509027]

[37]. Varghese A Reciprocal Modulation of I K1-I Na Extends Excitability in Cardiac Ventricular Cells. Front Physiol 2016;7:542. [PubMed: 27895596]

[38]. Schram G, Pourrier M, Wang Z, White M, Nattel S. Barium Block of Kir2 and Human Cardiac Inward Rectifier Currents: Evidence for Subunit-Heteromeric Contribution to Native Currents. Cardiovasc Res 2003;59:328–38. [PubMed: 12909316]

[39]. Preisig-Muller R, Schlichthorl G, Goerge T, Heinen S, Bruggemann A, Rajan S, et al. Heteromerization of Kir2.x potassium channels contributes to the phenotype of Andersen's syndrome. Proc Natl Acad Sci U S A 2002;99:7774–9. [PubMed: 12032359]

[40]. Miake J, Marban E, Nuss HB. Functional role of inward rectifier current in heart probed by Kir2.1 overexpression and dominant-negative suppression. J Clin Invest 2003;111:1529–36. [PubMed: 12750402]

[41]. Dangman KH, Danilo P Jr., Hordof AJ, Mary-Rabine L, Reder RF, Rosen MR. Electrophysiologic characteristics of human ventricular and Purkinje fibers. Circulation 1982;65:362–8. [PubMed: 7032748]

[42]. Akar FG, Nass RD, Hahn S, Cingolani E, Shah M, Hesketh GG, et al. Dynamic changes in conduction velocity and gap junction properties during development of pacing-induced heart failure. Am J Physiol Heart Circ Physiol 2007;293:H1223–30. [PubMed: 17434978]

[43]. Thomas SA, Schuessler RB, Berul CI, Beardslee MA, Beyer EC, Mendelsohn ME, et al. Disparate effects of deficient expression of connexin43 on atrial and ventricular conduction: evidence for chamber-specific molecular determinants of conduction. Circulation 1998;97:686–91. [PubMed: 9495305]

[44]. Lemoine MD, Krause T, Koivumaki JT, Prondzynski M, Schulze ML, Girdauskas E, et al. Human Induced Pluripotent Stem Cell-Derived Engineered Heart Tissue as a Sensitive Test System for QT Prolongation and Arrhythmic Triggers. Circ Arrhythm Electrophysiol 2018;11:e006035. [PubMed: 29925535]

[45]. Yoshinaga D, Baba S, Makiyama T, Shibata H, Hirata T, Akagi K, et al. Phenotype-Based High-Throughput Classification of Long QT Syndrome Subtypes Using Human Induced Pluripotent Stem Cells. Stem Cell Reports 2019;13:394–404. [PubMed: 31378668]

[46]. Zhang M, D'Aniello C, Verkerk A, Wrobel E, Frank S, Ward-van Oostwaard D, et al. Recessive Cardiac Phenotypes in Induced Pluripotent Stem Cell Models of Jervell and Lange-Nielsen Syndrome: Disease Mechanisms and Pharmacological Rescue. Proc Natl Acad Sci U S A 2014;111:E5382–92.

[47]. Azarbayjani F, Danielsson B. Embryonic Arrhythmia by Inhibition of HERG Channels: A Common Hypoxia-Related Teratogenic Mechanism for Antiepileptic Drugs? Epilepsia 2002;43:457–68. [PubMed: 12027905]

[48]. Danielsson B, Skold A, Azarbayjani F. Class III Antiarrhythmics and Phenytoin: Teratogenicity Due to Embryonic Cardiac Dysrhythmia and Reoxygenation Damage. Curr Pharm Des 2001;7:787–802. [PubMed: 11375779]

[49]. Attwell D, Cohen I, Eisner DA. The effects of heart rate on the action potential of guinea-pig and human ventricular muscle. J Physiol 1981;313:439–61. [PubMed: 7277229]

[50]. Bjørnstad H, Tande PM, Lathrop DA, Refsum H. Effects of temperature on cycle length dependent changes and restitution of action potential duration in guinea pig ventricular muscle. Cardiovasc Res 1993;27:946–50. [PubMed: 8221783]

[51]. Gutstein DE, Morley GE, Tamaddon H, Vaidya D, Schneider MD, Chen J, et al. Conduction slowing and sudden arrhythmic death in mice with cardiac-restricted inactivation of connexin43. Circ Res 2001;88:333–9. [PubMed: 11179202]

[52]. Danik SB, Liu F, Zhang J, Suk HJ, Morley GE, Fishman GI, et al. Modulation of cardiac gap junction expression and arrhythmic susceptibility. Circ Res 2004;95:1035–41. [PubMed: 15499029]

[53]. Magyar J, lost N, Körtvély A, Bányász T, Virág L, Szigligeti P, et al. Effects of endothelin-1 on calcium and potassium currents in undiseased human ventricular myocytes. Pflugers Arch 2000;441:144–9. [PubMed: 11205054]

[54]. Drouin E, Lande G, Charpentier F. Amiodarone reduces transmural heterogeneity of repolarization in the human heart. J Am Coll Cardiol 1998;32:1063–7. [PubMed: 9768733]

Highlights

- T3+Dex treatment increases I_{Na}, I_{K1}, I_{Kr} and I_{Ks} and reduces I_f in hiPSC-CMs.
- T3+Dex treatment shortens action potential in hiPSC-CMs.
- T3+Dex treatment increases conduction velocity in hiPSC-CM cell sheets.
- T3+Dex treatment enhances the electrophysiological maturation of hiPSC-CMs.

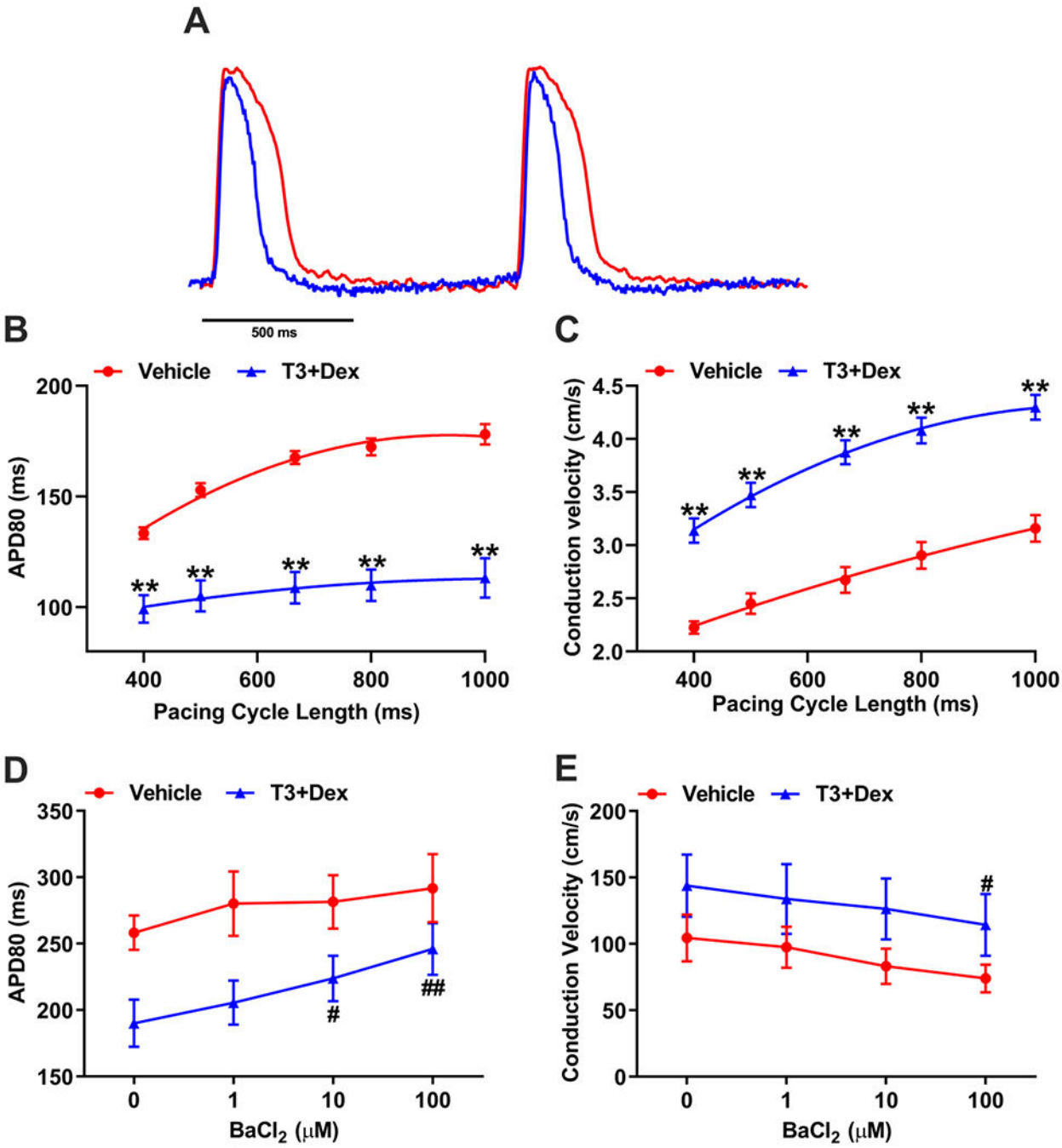

Fig. 1. Optical action potential measurements in vehicle- and T3+Dex-treated hiPSC-CM cell sheets (hiPSC-CCSs).

(**A**) Representative optical action potential records from FluoVolt-loaded hiPSC-CCSs at a pacing cycle length of 1000 ms (1 Hz). T3+Dex-treated hiPSC-CCSs had a shorter action potential duration at 80% repolarization (APD_{80}, **B**) and faster conduction velocity (**C**) than the vehicle at each pacing cycle lengths. N = 10 hiPSC-CCSs per group, collected from 3 independent biological experiments. At 1 Hz pacing, I_{K1} blockade by $BaCl_2$ significantly prolonged APD_{80} (**D**) and slowed down conduction velocity (**E**) in T3+Dex-treated hiPSC-

CCSs. N = 6 hiPSC-CCSs per group, collected from 3 independent biological experiments. Data were presented as mean ± SEM. Statistical difference was determined by two-way ANOVA with Sidak's multiple comparisons test between vehicle and T3+Dex and Dunnett's multiple comparisons test in the related group. * $p < 0.05$ and ** $p < 0.01$ compared with the vehicle. # $p < 0.05$ and ## $p < 0.01$ compared with the related group before $BaCl_2$ treatment.

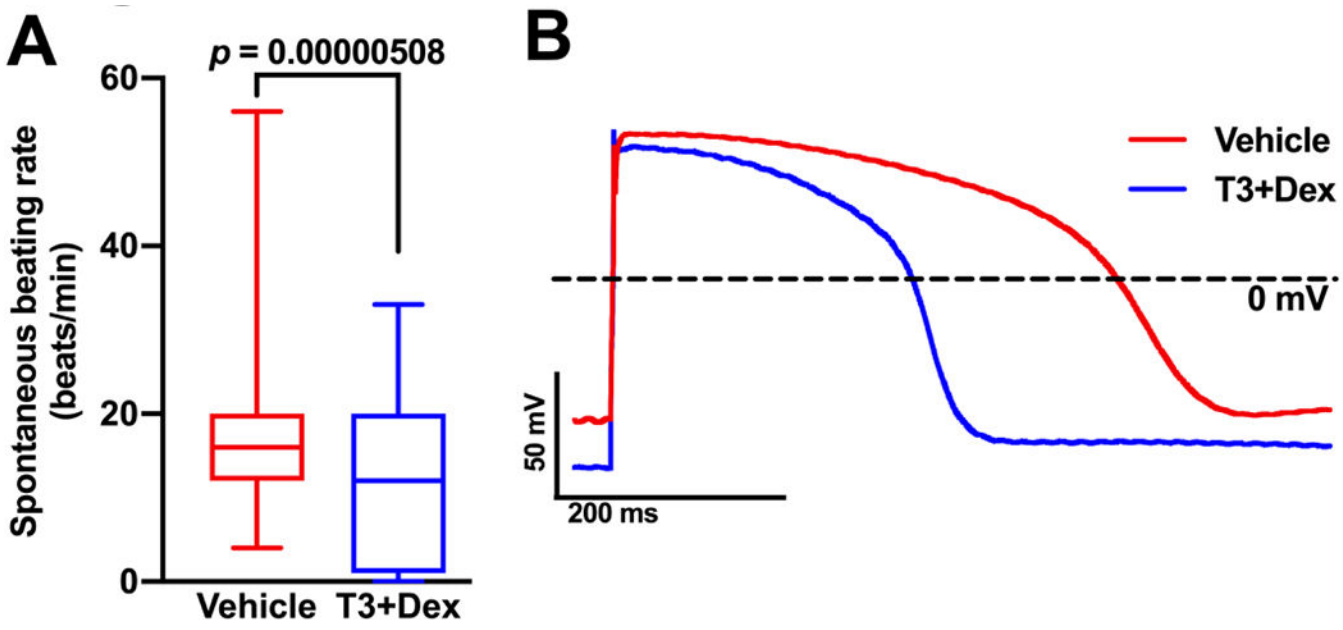

Fig. 2. Spontaneous beating rates and action potentials of single hiPSC-CMs.

(**A**) Average spontaneous beating rate of vehicle and T3+Dex-treated single hiPSC-CMs. Vehicle, n = 113 cells; T3+Dex, n= 135 cells. Data were represented as mean ± SEM of 2 independent biological experiments. Statistical difference was determined by unpaired two tailed t test.

(**B**) Representative action potentials recorded in vehicle- and T3+Dex-treated hiPSC-CMs at room temperature and 0.5 Hz pacing.

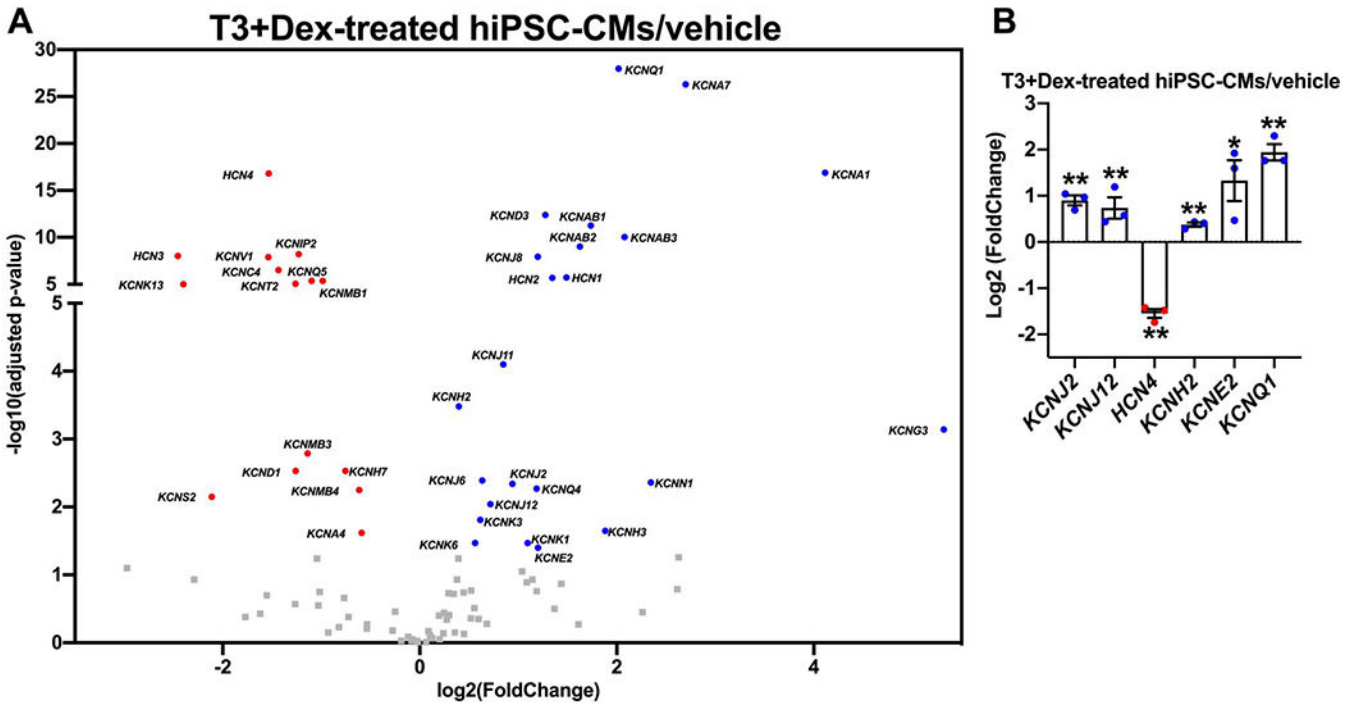

Fig. 3. RNA sequencing revealed change in the expression of potassium channel-related genes in T3+Dex-treated hiPSC-CMs.

(**A**) Volcano plot of potassium-channel genes. RNA sequencing was performed in vehicle- and T3+Dex-treated hiPSC-CMs (n = 3 independent biological replicates per group). Significantly down-regulated genes in T3+Dex-treated hiPSC-CMs are indicated in red, and up-regulated genes in blue. Genes with adjusted *p*-value >0.05 in grey.

(**B**) RNA sequencing results showed one downregulated gene (*HCN4*) and 5 upregulated genes (*KCNJ2*, *KCNJ12*, *KCNH2*, *KCNE2* and *KCNQ1*) important for cardiac automaticity and repolarization. * $p < 0.05$ and ** $p < 0.01$ compared with the vehicle.

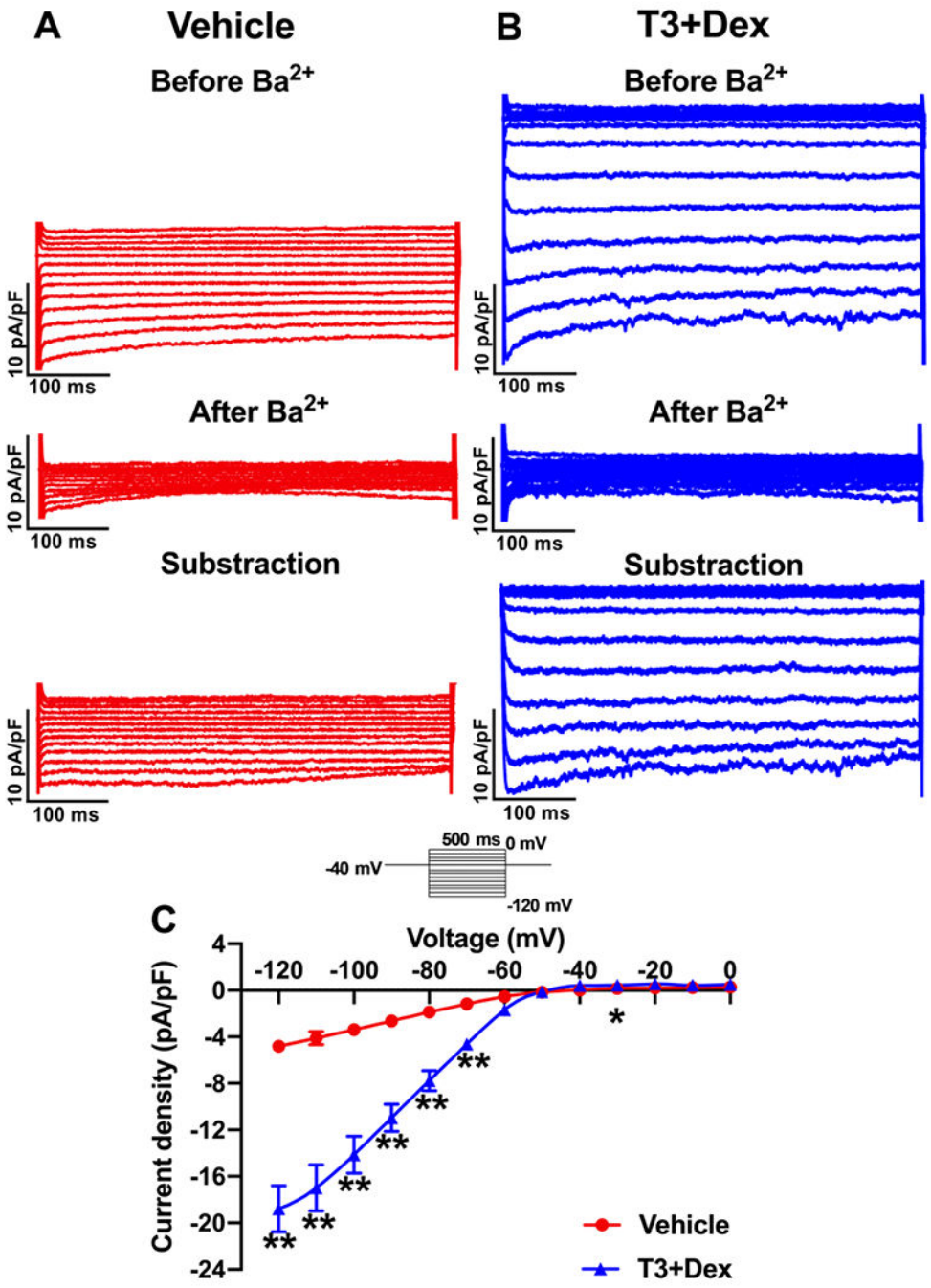

Fig. 4. Characteristics of inward rectifier potassium (I_{K1}) current in vehicle- and T3+Dex-treated hiPSC-CMs.

(**A**),(**B**) Representative records of I_{K1} normalized to cell capacitance. Top, middle and bottom traces: control, 0.5 mmol/L $BaCl_2$ treatment, and $BaCl_2$-subtraction, respectively. (**C**) Current-voltage (*I-V*) plot. Vehicle, n = 15 cells; T3+Dex, n = 11 cells. Data were represented as mean ± SEM of 3 independent biological experiments. Statistical difference was determined by two-way ANOVA with Sidak's multiple comparisons test between vehicle and T3+Dex. * $p < 0.05$ and ** $p < 0.01$ compared with the vehicle.

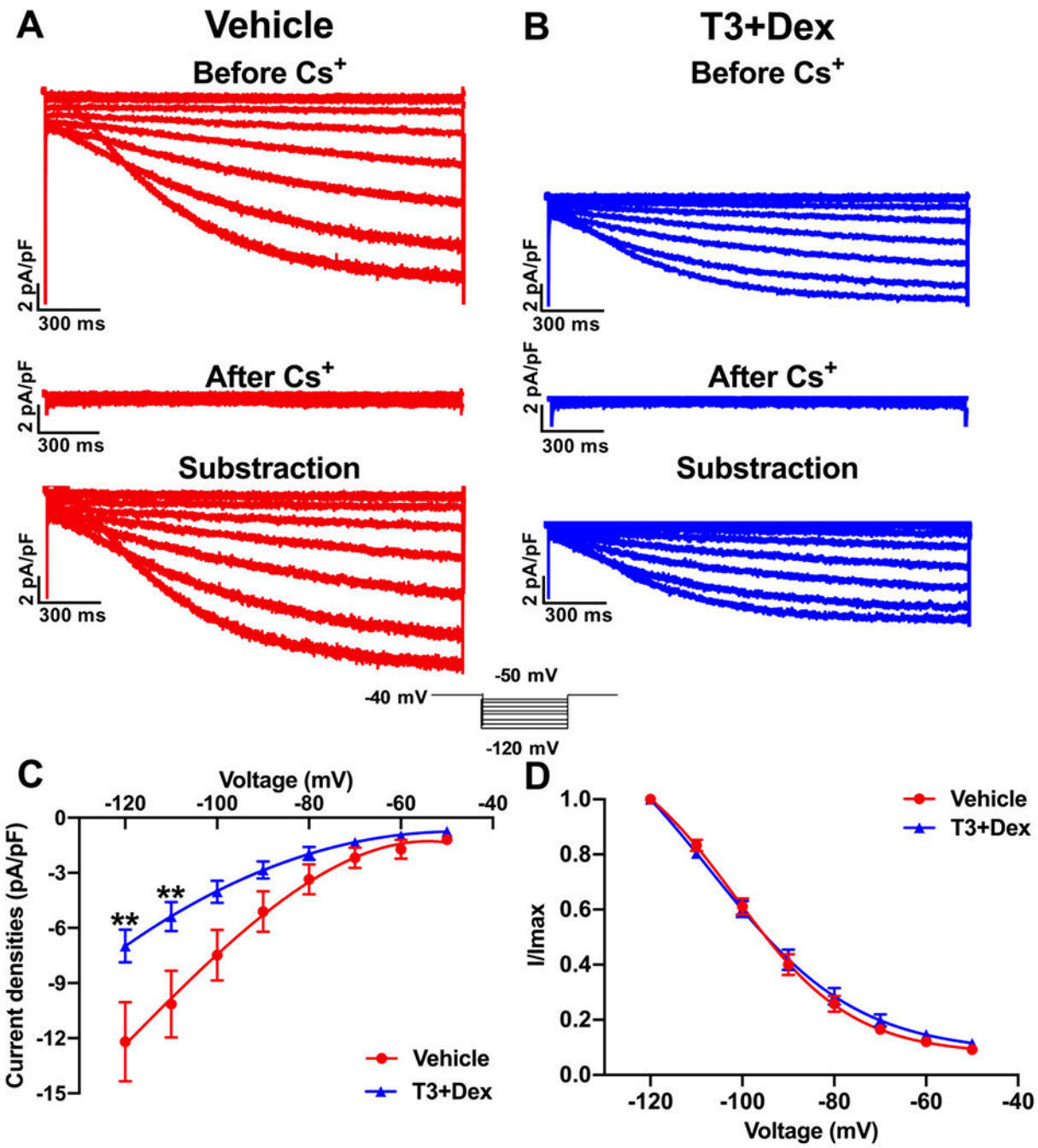

Fig. 5. Characteristics of funny current (I_f) in vehicle- and T3+Dex-treated hiPSC-CMs.

(**A**),(**B**) Representative records of I_f normalized to cell capacitance. Top, middle and bottom traces: control, 5 mmol/L CsCl treatment, and CsCl-subtraction, respectively.

(**C**),(**D**) Current-voltage (*I-V*) plot and activation curve of I_f. Vehicle, n = 14 cells; T3+Dex, n = 15 cells. Data were represented as mean ± SEM of 3 independent biological experiments. Statistical difference was determined by two-way ANOVA with Sidak's multiple comparisons test between vehicle and T3+Dex. ** $p < 0.01$ compared with the vehicle.

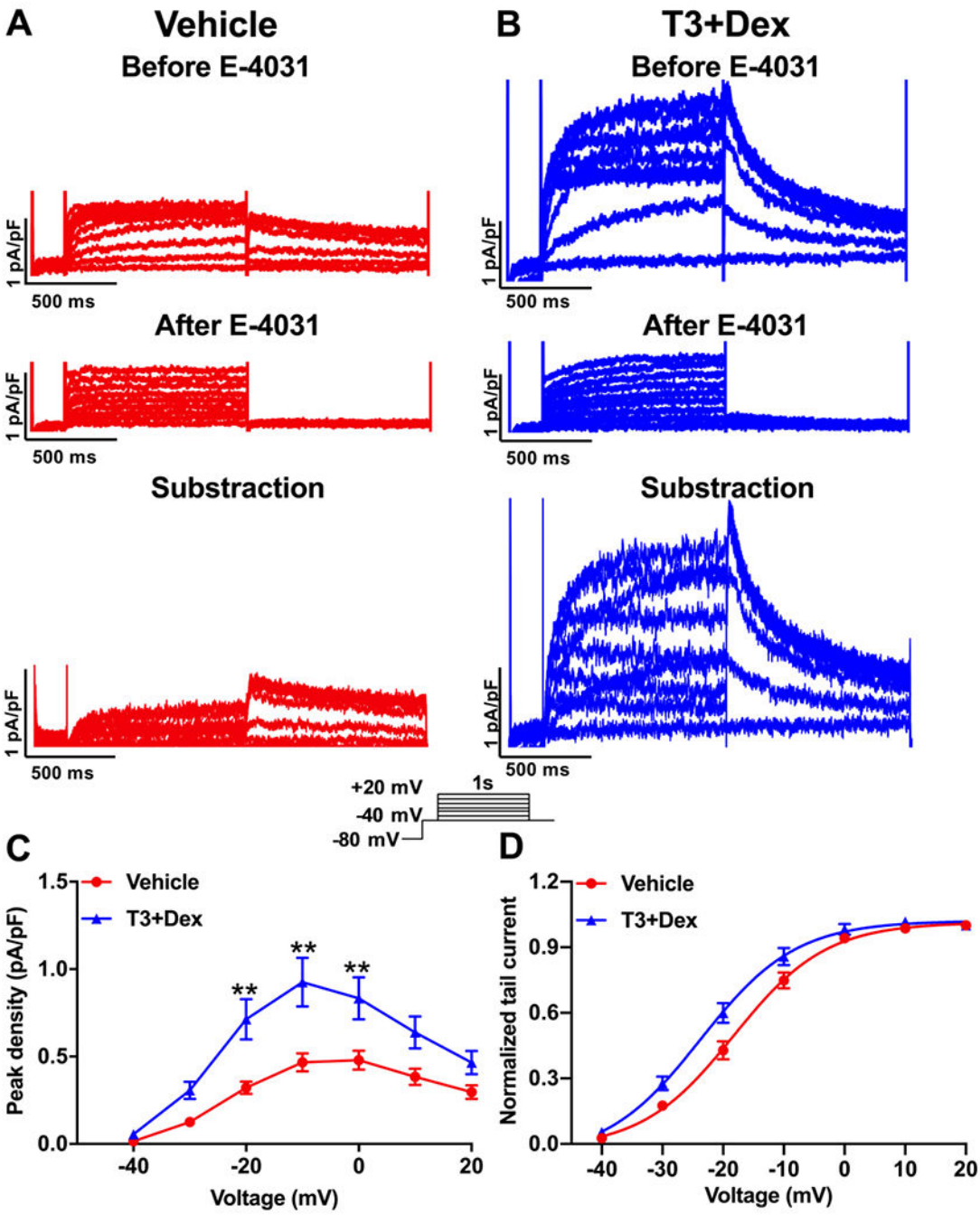

Fig. 6. Biophysical properties of rapidly delayed rectifier potassium current (I_{Kr}) in vehicle- and T3+Dex-treated hiPSC-CMs.

(**A**),(**B**) Representative records of I_{Kr} normalized to cell capacitance. Top, middle and bottom traces: control, 0.5 mmol/L E4031 treatment, and E4031-subtraction, respectively. (**C**),(**D**) Current-voltage (*I-V*) plot and activation curve of I_{Kr} during depolarization. Vehicle, n = 17 cells; T3+Dex, n = 18 cells. Data were represented as mean ± SEM of 3 independent biological experiments. Statistical difference was determined by two-way ANOVA with

Sidak's multiple comparisons test between vehicle and T3+Dex. ** $p < 0.01$ compared with the vehicle.

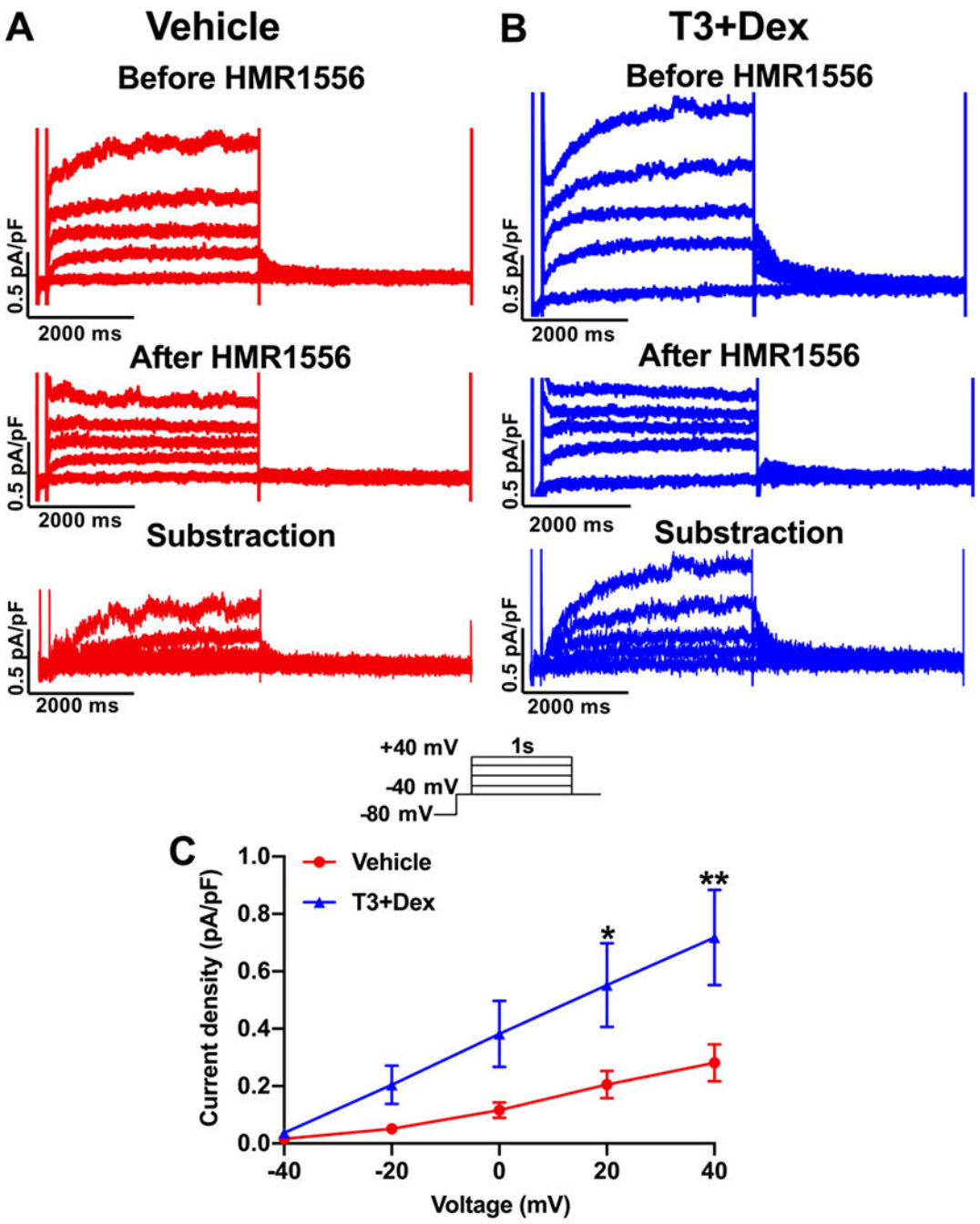

Fig. 7. Characteristics of the slow delayed rectifier potassium current (I_{Ks}) in T3+Dex- and vehicle-treated hiPSC-CMs.

(**A**), (**B**) Representative records of I_{Ks} normalized to cell capacitance. Top, middle and bottom traces: control, 0.5 mmol/L HMR1556 treatment and HMR1556-substraction, respectively.

(**C**) Current-voltage (*I-V*) plot. Vehicle, n = 9 cells; T3+Dex, n = 13 cells. Data were represented as mean ± SEM of 2 independent biological experiments. Statistical difference

was determined by two-way ANOVA with Sidak's multiple comparisons test between vehicle and T3+Dex. * $p < 0.05$ and ** $p < 0.01$ compared with the vehicle.

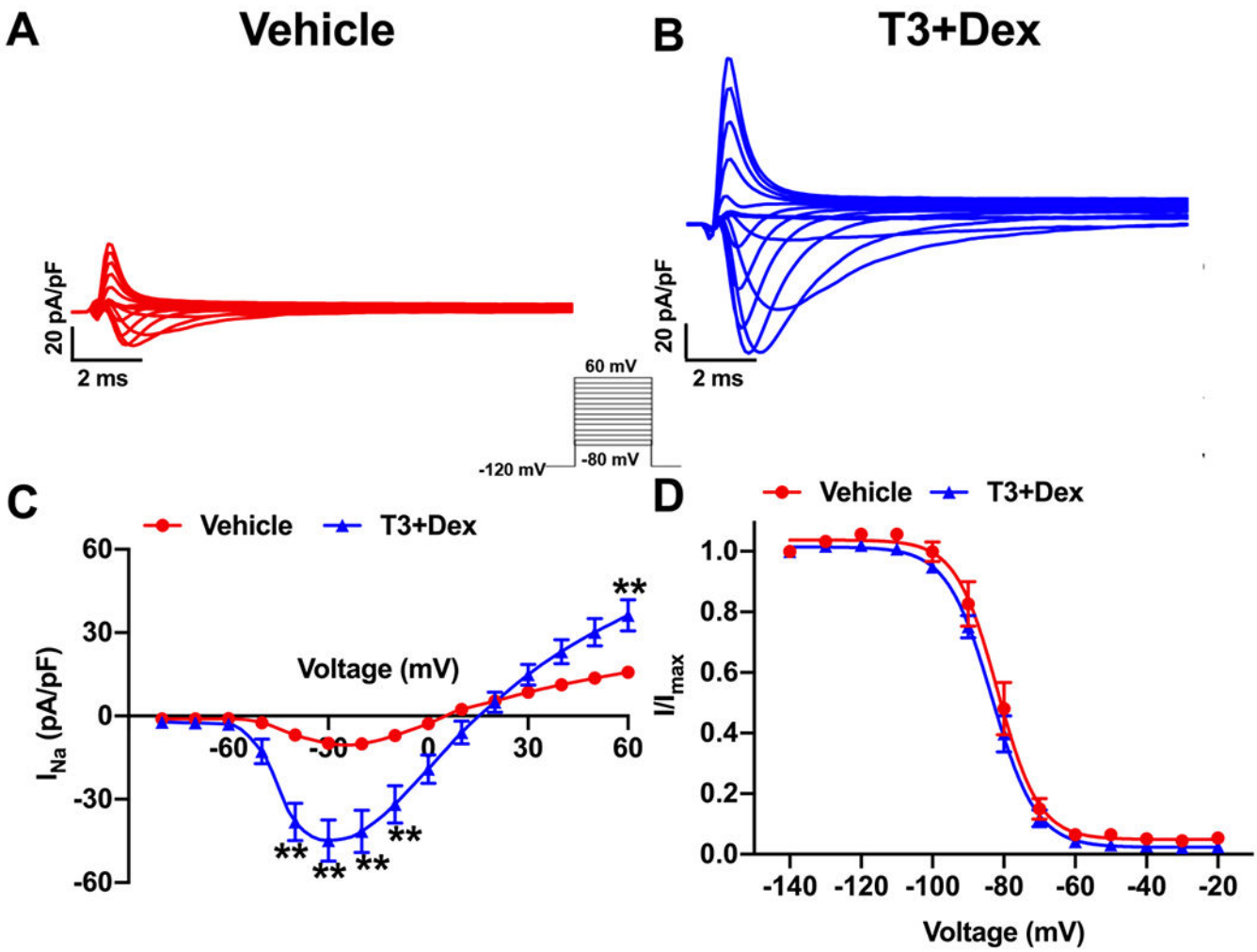

Fig. 8. Characteristics of sodium currents (I_{Na}) in vehicle- and T3+Dex-treated hiPSC-CMs.

(**A**),(**B**) Representative records of I_{na} normalized to cell capacitance.

(**C**),(**D**) Current-voltage (*I-V*) plot and steady-state inactivation of I_{Na}. Vehicle, n = 7 cells; T3+Dex, n = 9 cells. Data were represented as mean ± SEM of 2 independent biological experiments. Statistical difference was determined by two-way ANOVA with Sidak's multiple comparisons test between vehicle and T3+Dex. ** $p < 0.01$ compared with the vehicle.

Table 1.

Action potential characteristics of vehicle- and T3+Dex-treated hiPSC-CMs.

	Vehicle	T3+Dex	*p* value
Resting membrane potential (mV)	−65.04 ± 1.20	−72.00 ± 1.10	0.00008
Amplitude (mV)	119.43 ± 2.18	125.40 ± 1.60	0.028
Overshoot (mV) (Between 0 mV and the peak of action potential)	54.39 ± 1.83	53.40 ± 1.58	0.685
V_{max} (mV/ms)	86.08 ± 8.12	131.78 ± 8.49	0.0003
APD_{50} (ms)	367.69 ± 21.61	255.76 ± 11.58	0.00001
APD_{90} (ms)	550.44 ± 39.54	418.59 ± 21.58	0.003

Note: Vehicle, n = 25 cells; T3+Dex, n = 31 cells. Data were represented as mean ± SEM of 3 independent biological experiments. Statistic difference was determined by unpaired two tailed t test.